

Multivariate Bayesian Analysis of Atmosphere-Ocean General Circulation Models

Reinhard Furrer, Stephan R. Sain, Douglas Nychka, Gerald A Meehl

Presented by: Xuan Li

April, 2009

1. Introduction

Numerical experiments based on atmosphere–ocean general circulation models (AOGCMs) are one of the primary tools in deriving projections for future climate change. This article mainly focus on combining present day observations, present day and future climate projections in a single highdimensional hierarchical Bayes model for future predictions. The data source is from the Coupled Model Intercomparison Project (CMIP) and consists of 9 AOGCMs on a 2.8 by 2.8 degree grid under several different emission scenarios. The climate variables in this article are the average surface temperature and precipitation for the boreal winter (December, January and February, DJF) and boreal summer (June, July and August, JJA).

2. Methods

2.1 Random effects statistical model

The main points come from a random effects statistical model. From N climate models, X_i denotes a vector of average temperatures representing current climate at a grid of points on the surface of the Earth for the i th model. Y_i denotes the corresponding averages simulated at a future period under a specific scenario of climate change. Let $D_i = Y_i - X_i$, then

$$D_i = M\theta_i + \varepsilon_i,$$

where M is a matrix of spatial basis functions and θ_i is a random effect whose expected value is the true difference in climate. ε_i is assumed to be a mean zero spatial process which does not act in a single point but gradually spread influences all over the sphere.

2.2 Climate model data

As mentioned in the first section, the data are from 9 AOGCMs based on Coupled Model Intercomparison Project (CMIP). Here the variables that drive the climate are called *forcings*, such as greenhouse gases produced by human activities, changes in the sun's energy or changes in land use. CMIP has the data from "control runs", in which the forcing is considered as a constant at the

current level. It also collects data from “transient runs”, where the forcing is under certain idealized scenario of global warming.

Compared to temperature fields, the precipitation fields exhibit a different pattern. The spatial structures have smaller scales and the fields are more heterogeneous. Therefore, a log transformation is used to correct the shortcomings

2.3 Hierarchical Bayes approach

The temperature or log precipitation fields of the $N = 9$ models are stacked into vectors of length n , denoted as follows:

X_i = climatological field from control run of model i ,

Y_i = climatological field from transient run of model i .

The difference is given by: $D_i = Y_i - X_i$, $i = 1, \dots, N$, which represents the climate change with respect to temperature or log precipitation.

They use a standard hierarchical Bayes approach based on the following three levels: data, process, and priors.

For the *data level*, the climate change is a decomposition of a large scale climate signal and small scale signals consisting of model bias and internal model variability. Hence,

$$D_i = \mu_i + \varepsilon_i, [D_i | \mu_i, \phi_i] \sim N_n(\mu_i, \phi_i \Sigma), \phi_i > 0, i = 1, \dots, N,$$

where N_n is an n -dimensional normal density. Σ is specified and ϕ_i are scale parameters.

For the *process level*, μ_i , $i=1,2,\dots,9$ denote the large scale climate signals. They use a dimension reduction technique and assume that $\mu_i = M\theta_i$, where the given “design” matrix M contains p

basis functions with $p \ll n$. The “true” large scale climate change pattern is denoted as $M\mathcal{G}$,

and the θ_i are modeled as:

$$[\theta_i | \mathcal{G}, \psi_i] \sim N_p(\mathcal{G}, \psi_i \Omega), \psi_i > 0, i = 1, \dots, N,$$

where ψ_i are scale parameters. The correlation matrix Ω might have arbitrary structure, and

setting $\Omega = I$ would be a reasonable choice.

The last level puts priors on the process parameters:

$$[\phi_i] \sim I\Gamma(\xi_1, \xi_2), \xi_1, \xi_2 > 0, i = 1, \dots, N;$$

$$[\psi_i] \sim I\Gamma(\xi_3, \xi_4), \xi_3, \xi_4 > 0, i = 1, \dots, N;$$

$$[\mathcal{G}] \sim N_p(0, \xi_5 I), \xi_5 > 0;$$

where $I\Gamma$ denotes the inverse Gamma density and ξ_1, \dots, ξ_5 are hyperparameters.

2.4 Choice of basis functions

Basis functions are used to construct the design matrix M . These functions need to be sufficiently flexible to represent the mean structure of the difference fields. They use a technique called spherical harmonic. In a mathematical manner, spherical harmonics are the angular portion of an orthogonal set of solutions to Laplace's equation represented in a system of spherical coordinates. They are a generalization of a sin-cosine decomposition of a real valued function to the sphere. It is therefore natural

to assume that the large scale signal is a linear combination of p_s spherical harmonics. The spherical harmonics can be obtained with an iterative procedure and each additional level has smaller scales. In Fig. 5, the first spherical harmonics corresponds to the global mean ($l=0$), level $l=1$ consists of three single sin/cosine structures on the sphere and so on.

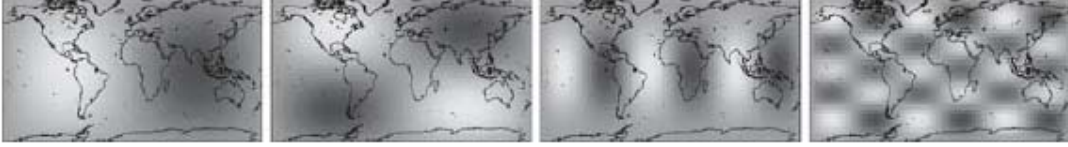


Fig. 5 Examples of spherical harmonics. The fields correspond to spherical harmonics from levels $l = 1, 2, 3, 7$



Fig. 6 Examples of land indicator basis functions. From left to right Alaska, Greenland, Canadian arctic ice and lower USA

Since these patterns based on land forms are not easily represented by spherical harmonics, they also use indicator basis functions linked to land forms and sea ice, see Fig.6.

2.5 Correlation matrices and correlation function

Assume that ε_i are isotropic and stationary processes on the sphere. It means that covariance between these two points only depends only on the great circle distance θ . This assumption is supported on a global scale by exploratory graphical analysis with ε_i (Cressie 1993).

They used Poisson kernel and exponential correlation function in this article. The formulas are as following:

$$c(\theta; \eta) = \frac{(1-\eta)^2(1-\eta^2)}{(1+\eta)(1-2\eta \cos(\theta) + \eta^2)^{3/2}}, \eta \in (0,1), \theta \in [0, \pi]$$

$$c(\theta; \tau) = \exp\left(\frac{-2R \sin(\theta/2)}{\tau}\right), \tau > 0, \theta \in [0, \pi]$$

2.6 Implementing a Gibbs sampler

Given the model observations D_i , the hierarchical modeling approach will construct the posterior distribution of $M\mathcal{Z}$. The posterior can be sampled using a Markov chain Monte Carlo (MCMC)

procedure known as the Gibbs sampler (Geman and Geman 1984; Gelfand and Smith 1990). The full conditionals are:

$$\begin{aligned}
 [\boldsymbol{\theta} | \dots] &\sim \mathcal{N}_p(\mathbf{A}^{-1}\mathbf{b}, \mathbf{A}^{-1}), \quad \mathbf{A} = \frac{1}{\xi_5} \mathbf{I} + \sum_{i=1}^N \frac{1}{\psi_i} \mathbf{I}, \quad \mathbf{b} = \sum_{i=1}^N \frac{1}{\psi_i} \boldsymbol{\theta}_i; \\
 [\boldsymbol{\theta}_i | \dots] &\sim \mathcal{N}_p(\mathbf{A}^{-1}\mathbf{b}, \mathbf{A}^{-1}), \quad \mathbf{A} = \frac{1}{\psi_i} \mathbf{I} + \frac{1}{\phi_i} \mathbf{M}^\top \boldsymbol{\Sigma}^{-1} \mathbf{M}, \quad \mathbf{b} = \frac{1}{\psi_i} \boldsymbol{\theta} + \frac{1}{\phi_i} \mathbf{M}^\top \boldsymbol{\Sigma}^{-1} \mathbf{D}_i; \\
 [\phi_i | \dots] &\sim \Pi\left(\xi_1 + \frac{n}{2}, \xi_2 + \frac{1}{2}(\mathbf{D}_i - \mathbf{M}\boldsymbol{\theta}_i)^\top \boldsymbol{\Sigma}^{-1}(\mathbf{D}_i - \mathbf{M}\boldsymbol{\theta}_i)\right); \\
 [\psi_i | \dots] &\sim \Pi\left(\xi_3 + \frac{p}{2}, \xi_4 + \frac{1}{2}(\boldsymbol{\theta}_i - \boldsymbol{\theta})^\top (\boldsymbol{\theta}_i - \boldsymbol{\theta})\right),
 \end{aligned}$$

3. Results

The simulation parameters and hyperparameters for the simulations are listed in Table 2. Range τ means the correlation range and s/n ratio means the signal/noise ratio. If more basis functions are included in M the resulting processes ε_i has a smaller spatial range. Figures 8 and 9 depict trace plots and kernel estimates of the posterior densities for the mean, the spherical harmonics, the NCEP climate observations and the land indicator fields given in Figs. 5 and 6 of the parameter $\boldsymbol{\theta}$.

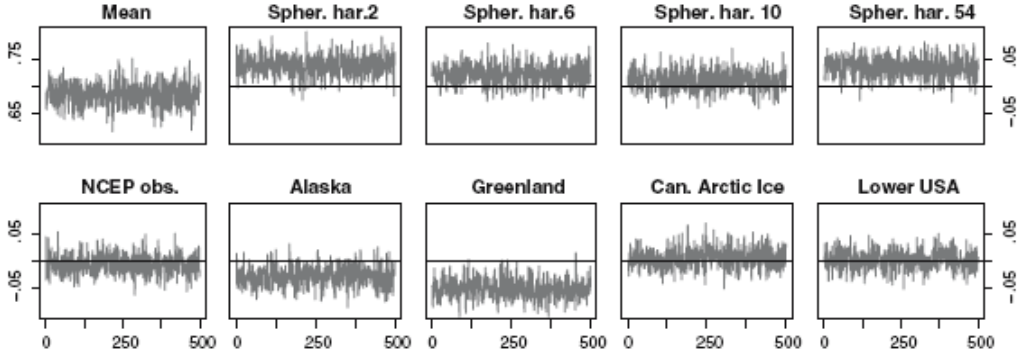


Fig. 8 Trace plots for the mean, the spherical harmonics given in Fig. 5 (top row), the NCEP climate observation and the land indicator fields given in Fig. 6 (bottom row) of the parameter $\boldsymbol{\theta}$ for the DJF temperature change. Note the different scales between the mean and the remaining panels

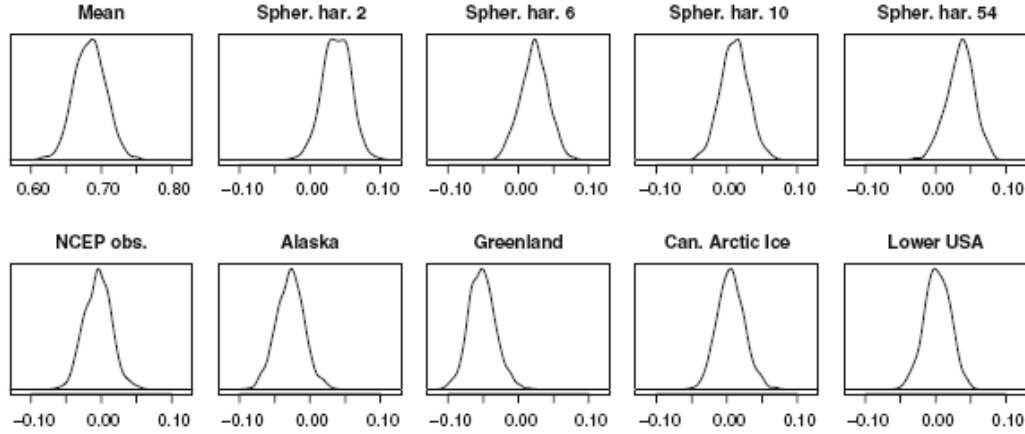


Fig. 9 Kernel estimates of the posterior densities for the mean, the spherical harmonics given in Fig. 5 (top row), the NCEP climate observation and the land indicator fields given in Fig. 6 (bottom row) of the parameter $\boldsymbol{\theta}$ for the DJF temperature change

Figure 10, 11 and 12 show the patterns of some analysis of surface temperature and precipitation fields. Figure 10 gives the temperature change that occurs with at least 80% probability in 70 years with 1% CO₂ increase. Figure 11 shows the probability that the temperature change exceeds 2°C. Figure 12 gives the median precipitation change that occurs in 70 years with 1% CO₂ increase.

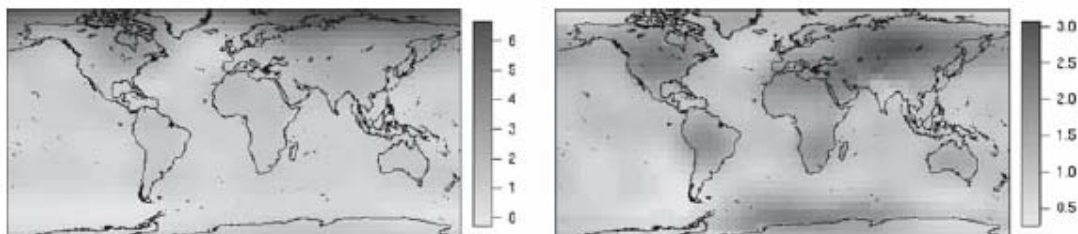


Fig. 10 The DJF (left panel) and JJA (right panel) temperature change (degree Celsius) that occurs with at least 80% probability in 70 years with 1% CO₂ increase.

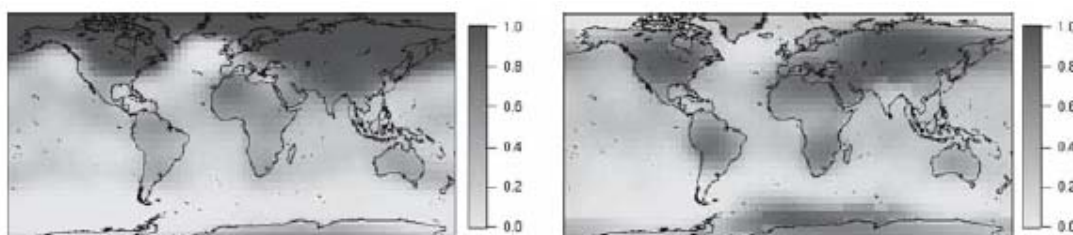


Fig. 11 Probability that DJF (left panel) and JJA (right panel) temperature change exceeds 2°C

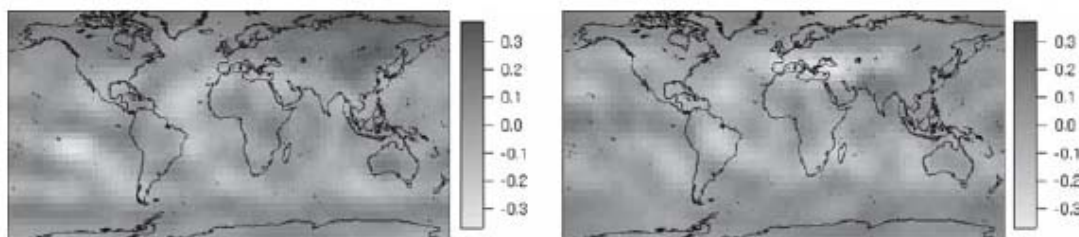


Fig. 12 The median DJF (left panel) and median JJA (right panel) log precipitation change (mm/day) that occurs in 70 years with 1% CO₂ increase

4. Model checking and extensions

Overall the realizations from the posterior look qualitatively similar to the actual model output. This agreement confirms the adequacy of the modeling approach. But there are some improvements that could be done. First, the covariance can be parameterized by modeling the range parameter and the signal to noise ratio in the Gibbs sampler. Second, since the new generation of model data for the Fourth Assessment Report (AR4) of the IPCC has several runs for different models, we can generate ensembles of runs and interpret them as multiple realizations of weather from the same climate. Third, there could be another approach which models the control and transient fields individually and linking them via a correlation structure.